between the g_2 values of the azole complexes and the $pK_a(BH^+)$ values of the azoles. Plots of the g_2 values in Table II against the $pK_a(BH^+)$ values are illustrated in Figure 2, in which the straight line was drawn by the least-squares method for the plots of unhindered azoles. The plots of hindered imidazoles (**3**, **9**, **10**, and **11**) are separately located to the upper side of the straight line, independent of their $pK_a(BH^+)$ values, which can correspond to the weakening of the iron to ligand bond due to the steric interaction with the porphyrin core.

The $pK_a(B)$ value of the coordinated azolates can be estimated from the g_2 values of the azolate complexes on the extrapolation of the straight line in Figure 2. The estimated $pK_a(B)$ values are 7-8 for tetrazolate, 8.5-9.5 for 1,2,4-triazolate and benzimidazolate, and 10-11 for imidazolate, 4-methylimidazolate, and 4-phenylimidazolate. Thus, the benzimidazole of a hindered imidazole and the tetrazole and 1,2,4-triazole of a weak base are transformed into a strong base on deprotonation of N_1H, and the deprotonation in unhindered imidazoles leads to a pK_a shift of 3-4 units. It is interesting that the magnitude of this increase in pK_a value at the N_3 position of the unhindered imidazoles is comparable to that of the shift in pK_a value for deprotonation at N_1H from free imidazole (14.44)[31] to coordinated imidazole in ferric porphyrin complex (10.4)[32] and metmyoglobin (10.34).[31]

The deprotonation of coordinated azole N_1H can weaken the iron to NO bond as described above, accompanying an increase in the basicity of donor nitrogen. The weakening of iron to NO bond may facilitate the dissociation of nitrosyl ligand. This is consistent with the result that the reaction of Fe(PPIXDME)(NO)(base) $\rightleftarrows$ Fe(PPIXDME)(base)$_2$ + NO proceeds to the right as the iron to NO bond strength in Fe(PPIXDME)(NO)(base) complex decreases.[20] Accordingly, it is probable that the deprotonation of proximal imidazole $N_\delta H$ in hemoproteins enhances the reactivity of the trans axial position, which coincides with the previous suggestions.[3,6,14]

Registry No. **2**, 85200-22-2; **3**, 100082-70-0; **4**, 100082-71-1; **5**, 71016-02-9; **6**, 100082-72-2; **11**, 100082-73-3; **12**, 100082-74-4; **13**, 100082-75-5; **14**, 100082-76-6; **15**, 100082-77-7; **16**, 100082-78-8; **17**, 85200-21-1; **18**, 100082-79-9; **19**, 100082-80-2; **20**, 100082-81-3; **21**, 100082-82-4; **22**, 100082-83-5; **23**, 100082-84-6; Fe(PPIXDME)Cl, 15741-03-4; Fe(PPIXDME)(NO), 58357-23-6.

(31) George, P.; Hannaia, G. I. H.; Irvine, D. H.; Abu-Issa, I. *J. Chem. Soc.* **1964**, 5689.
(32) Mohr, P.; Scheler, W.; Frank, K. *Naturwissenschaften* **1967**, *54*, 227.

Contribution from the Department of Chemistry, Case Western Reserve University, Cleveland, Ohio 44106

Kinetics of Ternary Complex Formation: The (Adenosine 5′-triphosphato)nickel(II) + 2,2′-Bipyridine System

K. J. Butenhof, D. Cochenour, J. L. Banyasz, and J. E. Stuehr*

Received October 1, 1985

The kinetics of formation of mixed-ligand complexes containing nickel(II), 2,2′-bipyridine, and adenosine 5′-triphosphate were studied by stopped-flow spectroscopy at 15 °C. A single relaxation effect was observed in the near-UV region. The pH and concentration dependencies of this effect were modeled most completely by three interconnected ternary formation steps. These steps correspond to the ternary complex formation of Ni(ATPH)(bpy), Ni(ATP)(bpy) and HONi(ATP)(bpy). The formation rate constants were found to be 1.9×10^3, 4.3×10^3, and 2.2×10^5 M^{-1} s^{-1} respectively. The magnitudes of these constants are interpreted in terms of statistical effects, labilization of inner-sphere water molecules, and chelation effects.

Introduction

Considerable interest has been focused on the thermodynamics and kinetics of ternary metal complexes because of the role these complexes play in biological systems. Although many biological systems that require a metal ion also require enzymes and cofactors, much simpler systems may serve to investigate fundamental metal-ligand interactions.

As a result of previous studies on binary and ternary systems, several factors have been identified that determine ternary complex formation rates: (1) the magnitude of the outer-sphere metal-ligand association constant, K_{os} (which varies greatly as a function of the association distance, ligand charge, metal charge, and bulk ionic strength);[1] (2) the rate of dissociation of inner-sphere water molecules (which is characteristic of a given metal but is dependent on the nature and number of bound ligands);[2-9] (3) the number of sites available for reaction;[10] (4) the preferred orientation of the available sites for a given incoming ligand.[11-13]

This paper presents an analysis of the formation rate constants for the ternary system Ni|ATP|bpy[14] for several concentrations over the pH range 4.5-8.5. Previous studies, with few exceptions,[15] have investigated the kinetics of ternary systems over a comparatively narrow pH range. We also present kinetic data for the component system Ni|bpy. Although this binary system has been studied previously by Wilkins and co-workers,[3] the method of analysis and the experimental conditions were different from those used in the present study.

Experimental Section

Materials. The concentrations of ca. 0.04 M $NiCl_2 \cdot 6H_2O$ (Fisher) stock solutions were determined by either atomic absorption or EDTA titration. Disodium adenosine 5′-triphosphate (Sigma) and 2,2′-bipyridine (Fisher) were used without further purification. All solutions were prepared with triply purified water containing 0.1 M KCl to maintain an approximately constant ionic strength. The stopped-flow solutions described below were prepared daily. A 0.001 M 2,2′-bipyridine stock solution was prepared weekly.

Equipment. The kinetic experiments were carried out on a Gibson-Durrum stopped-flow spectrometer thermostated at 15 °C. The concentration and pH range was also scanned by temperature-jump spectroscopy; no other effects were observed. A Corning digital potentiometer

(1) Frey, C. M.; Stuehr, J. E. "Metal Ions in Biological Systems"; Sigel, H., Ed.; Marcel Dekker: New York, 1974; Vol. 1, pp 51-116.
(2) Hunt, J. P. *Coord. Chem. Rev.* **1971**, *7*, 1-10.
(3) Holyer, R. H.; Hubbard, C. D.; Kettle, S. F. A.; Wilkins, R. G. *Inorg. Chem.* **1965**, *4*, 929-35.
(4) Pasternack, R. F.; Huber, P. R.; Huber, U. M.; Sigel, H. *Inorg. Chem.* **1972**, *11*, 276-80.
(5) Pasternack, R. F; Huber, P. R.; Huber, U. M.; Sigel, H. *Inorg. Chem.* **1972**, *11*, 420-2.
(6) Margerum, D. W.; Rosen, H. M. *J. Am. Chem. Soc.* **1967**, *89*, 1088-92.
(7) Jones, J. P.; Billo, E. J.; Margerum, D. W. *J. Am. Chem. Soc.* **1970**, *92*, 1875-80.
(8) Cobb, M. A.; Hague, D. N. *J. Chem. Soc., Faraday Trans. 1* **1972**, *68*, 932-39.
(9) Kowalak, A.; Kustin, K.; Pasternack, R. F.; Petrucci, S. *J. Phys. Chem.* **1967**, *89*, 3126-30.
(10) Sharma, V. S.; Schubert, J. *J. Chem. Educ.* **1969**, *46*, 506-7.
(11) Raycheba, J. M. T.; Margerum, D. W. *Inorg. Chem.* **1980**, *19*, 837-43.
(12) Sigel, H.; Huber, P. R.; Pasternack, R. F. *Inorg. Chem.* **1971**, *10*, 2226-8.
(13) Farrar, D. T.; Stuehr, J. E.; Moradi-Araghi, A.; Urbach, F. L.; Campbell, T. G. *Inorg. Chem.* **1973**, *12*, 1847-51.
(14) Ni|ATP|bpy refers to the *system* containing nickel(II), ATP, and bipyridine as a whole. Ni(ATP)(bpy) refers to a specific complex.
(15) There are of course several exceptions, for example: Sharma, V. S.; Leussing, D. L. *Inorg. Chem.* **1972**, *11*, 138-43.

0020-1669/86/1325-0691$01.50/0

Table I. Logarithms of Stability Constants for Binary and Ternary Interactions[a]

	Ni^{2+}	$NiOH^{+}$	$HATP^{3-}$	ATP^{4-}	bpy	$Ni(bpy)^{2+}$
H^{+}		10.2[b]	4.18[j,k]	6.57[j,k]	4.40[c]	
ATP^{4-}	4.79[j,k]	5.36[i,l]		0.11[e]	0.91[f]	4.50[f,i]
bpy	7.31[c]			0.91[f]	0.78[g]	7.10[c]

other interactions	log K
$Ni(bpy)_2^{2+} + bpy = Ni(bpy)_3^{3+}$	6.43[c]
$Ni(ATP)^{2-} + Ni^{2+} = Ni_2(ATP)$	2.40[d]
$Ni^{2+} + ATPH^{3-} = Ni(ATPH)^{-}$	2.78[j,k]
$Ni(ATP)(bpy)^{2-} + H^{+} = Ni(ATPH)(bpy)^{-}$	2.5[h]
$HONi(ATP)(bpy)^{3-} + H^{+} = Ni(ATP)(bpy)^{2-}$	10[h]

[a] Determined at or corrected to 15 °C and I = 0.1 M. [b] Reference 21. [c] Stability constant and ΔH values from ref 22. [d] Reference 16. [e] Reference 19. [f] Reference 18. [g] Reference 20. The (bpy)(bpy) stacking stability constant is included for completeness, but it has a negligible effect on the kinetics for our experimental conditions. [h] Determined in this paper; see text. [i] ΔH estimated from ref 21 and 23. [j] Reference 17. [k] ΔH values from ref 23. [l] Reference 29.

and either a Beckman combination electrode or an Orion combination electrode were used for pH measurements.

Preparation of Stopped-Flow Solutions. For the binary (Ni|bpy) and ternary (Ni|ATP|bpy) systems, solutions A and B were mixed in equal volumes. The preparation of the stopped-flow solutions were analogous for the binary and ternary systems; therefore, only the preparation of the ternary solutions is described.

(1) Solution A (ATP|bpy). Na_2ATP was dissolved in 0.1 M KCl, and the solution was adjusted to pH 7.1. Then bpy stock solution and 0.1 M KCl were added as the final pH was adjusted.

(2) Solution B (Ni|ATP). Na_2ATP was dissolved in 0.1 M KCl, and the solution was adjusted to pH 7.8. Then a ca. 0.04 M stock $NiCl_2$ solution and 0.1 M KCl was added. The final pH was adjusted to match that of solution A.

Stability Constants. Several of the equilibrium constants necessary to describe the Ni|ATP|bpy and Ni|bpy systems have been determined by Frey and Stuehr at 15 °C.[16,17] Others were extrapolated[18-20] from 25 °C, by using known[21-23] or estimated ΔH values. The values of the two previously unreported equilibrium constants for Ni(ATPH)(bpy) = Ni(ATP)(bpy) + H^{+} and Ni(ATP)(bpy) = HONi(ATP)(bpy) + H^{+} were obtained by iteration, as described below. All equilibrium constants are given in Table I.

Treatment of Data. All solutions displayed a single first-order relaxation effect in the near-UV region. The time constants of the observed exponential relaxation were analyzed from photographs of oscilloscope traces by standard semilogarithmic graphical techniques. In addition, a Biomation 802 transient recorder stored traces for computer analysis by the program STEAM via a modified Marquardt algorithm.[24]

The kinetic expressions were derived on the basis that all of the relaxation traces were simple exponential decays.[25] The unknown rate and equilibrium constants were varied to minimize χ^2 for the experimental $1/\tau$ data by using an estimated standard deviation of 10%.

The best-fit forward rate constants (k_f) are composed of an outer-sphere association constant (K_{os}) and an effective first-order rate constant:

$$k_f = K_{os}k_{eff} \quad (1)$$

The constant k_{eff} is useful in interpreting the variations found among the forward rate constants determined in this study. Under certain conditions k_{eff} reduces to the water dissociation rate constant (k_w) for the reactant metal complex.

The value of K_{os} can be calculated[26,27] from

$$K_{os} = 4\pi SNa^3e^{-U/kT}/3000 \qquad S = S_M S_L \quad (2)$$

Scheme I

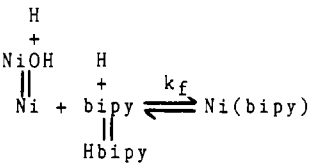

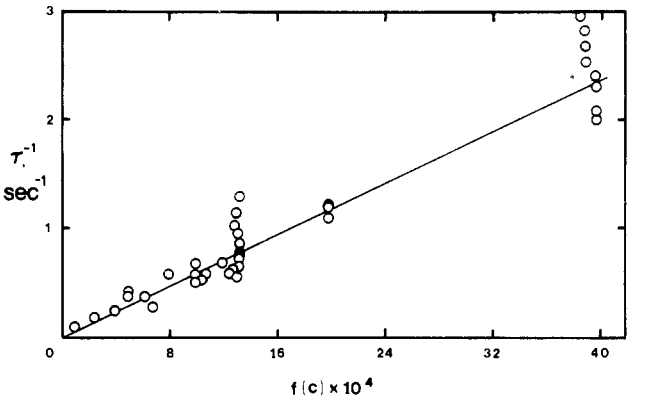

Figure 1. Variation of the Ni(ATP), relaxation time ($1/\tau$) with pH, $[Ni]_0$, and $[bpy]_0$. Experimental data points are indicated with circles, the solid line is calculated from eq 3.

where a is the outer-sphere separation parameter and U is the electrostatic potential (which is equal to zero in this study because bpy is uncharged). The variables S_M and S_L are geometric factors associated with the reactant metal complex and the ligand respectively. The value of S is approximated by the fraction of surface area of each reactant that is active in the reaction; for the interaction of two spheres S = 1. Ionic strength corrections to K_{os}, which are generally important, are approximately equal to unity in this study because bpy is uncharged. We have used a value of 0.1S for K_{os}, which corresponds to a value of 3.5 Å for a.

Results

Binary (Ni|bpy). For Ni|bpy, a single relaxation effect was observed at ca. 300 nm. The data given in Table II cover pH 4.5–8.5 for a wide range of Ni(II) and bpy concentrations. The mechanism that most closely describes the kinetic data over these conditions is shown in Scheme I. This mechanism involves the slow formation of Ni(bpy) coupled to two rapid proton-transfer reactions.

The reciprocal relaxation time is given by

$$1/\tau = k_f\frac{[Ni]([H][bpy] + K_{Hbpy}X) + [bpy]([H]Y + K_{Hbpy}[NiOH])}{X(K_{Hbpy} + [H]) + [bpy](K_{NiOH} + [H])} + k_r \quad (3)$$

where $X = K_{NiOH} + [NiOH] + [H]$, $Y = K_{Hbpy} + [bpy] + [H]$, and [H], [bpy], [Ni], and [NiOH] represent equilbrium concentrations. A variety of other mechanisms were modeled and rejected, including several involving hydroxo species. A graph of $1/\tau$ vs. the concentration term in eq 3 is shown in Figure 1. Our value for the Ni(bpy) formation rate constant (k_f) of 590 M^{-1} s^{-1} at 15 °C compares well with the value of 610 M^{-1} s^{-1} at 15 °C determined by Wilkins and co-workers.[3]

Ternary (Ni|ATP|bpy). A single kinetic effect was observed in the near-UV region for the ternary system over a wide pH range (4–8) for different total Ni(II) and bpy concentrations at 15 °C and I = 0.1 M. This effect was quite sensitive to the pH and Ni(II) concentrations. Figure 2a shows the experimental $1/\tau$ data and the calculated curve, where both are plotted vs. the equilibrium concentration of Ni(bpy).[28] Three distinct curves are apparent in Figure 2a; these correspond to the variations of $1/\tau$ with

(16) Frey, C. M.; Stuehr, J. E. *J. Am. Chem. Soc.* **1978**, *100*, 139–45.
(17) Frey, C. M.; Stuehr, J. E. *J. Am. Chem. Soc.* **1972**, *94*, 8898–904.
(18) Chaudhuri, P.; Sigel, H. *J. Am. Chem. Soc.* **1977**, *99*, 3142–50.
(19) Mitchell, P. R.; Sigel, H. *Eur. J. Biochem.* **1978**, *88*, 149–54.
(20) Tripolet, R.; Malini-Balakrishnan, R.; Sigel, H. *J. Chem. Soc., Dalton Trans.*, in press.
(21) Perrin, D. D. *J. Chem. Soc.* **1964**, 3644–8.
(22) Anderegg, G. *Helv. Chem. Acta* **1963**, *46*, 2813–22.
(23) Taqui Khan, M. M.; Martell, A. E. *J. Am. Chem. Soc.* **1966**, *88*, 668–71.
(24) Marquardt, D. W. *J. Soc. Ind. Appl. Math.* **1963**, *11*, 431–41.
(25) Bernasconi, C. F. "Relaxation Kinetics"; Academic Press: New York, 1976.
(26) Fuoss, R. M. *J. Am. Chem. Soc.* **1958**, *80*, 5059–61.
(27) Eigen, M. *Z. Phys. Chem. (Munich)* **1954**, *1*, 176–200.
(28) This species was chosen arbitrarily; it shows the most dramatic changes of $1/\tau$ as a function of pH and metal ion concentrations.

Table II. Kinetic Data for the Interaction of Ni(II) with bpy[a]

$[Ni]_0$, mM	$[bpy]_0$, mM	pH[b]	$1/\tau$, s^{-1} exptl	$1/\tau$, s^{-1} calcd
4.00	0.05	7.00	2.60	2.31
4.00	0.05	7.00	2.50	2.31
4.00	0.01	7.05	2.30	2.34
4.00	0.02	7.05	2.40	2.33
4.00	0.05	7.05	2.70	2.31
4.00	0.07	7.05	2.80	2.30
4.00	0.01	7.07	2.00	2.34
2.00	0.01	7.07	1.10	1.17
1.00	0.01	7.07	0.58	0.58
0.50	0.01	7.08	0.42	0.29
0.50	0.01	7.07	0.42	0.29
0.25	0.01	7.07	0.21	0.14
0.10	0.01	7.07	0.10	0.05
1.33	0.01	8.78	1.03	0.75
1.33	0.01	8.75	0.97	0.75
1.33	0.01	8.60	1.15	0.76
1.33	0.01	8.42	0.96	0.77
1.33	0.01	7.66	0.86	0.77
1.33	0.01	7.59	1.30	0.77
1.33	0.01	7.45	0.87	0.77
1.33	0.01	7.38	0.82	0.77
1.33	0.01	7.30	0.77	0.77
1.33	0.01	7.22	0.77	0.77
1.33	0.01	7.20	0.74	0.77
1.33	0.01	7.14	0.80	0.77
1.33	0.01	7.13	0.72	0.77
1.33	0.01	7.01	0.65	0.77
1.33	0.01	6.98	0.77	0.77
1.33	0.01	6.63	0.78	0.77
1.33	0.01	6.21	0.56	0.76
1.33	0.01	6.21	0.56	0.76
1.33	0.01	6.07	0.74	0.76
1.33	0.01	5.92	0.63	0.75
1.33	0.01	5.67	0.59	0.73
1.33	0.01	5.45	0.69	0.70
1.33	0.01	5.10	0.59	0.62
1.33	0.01	5.06	0.53	0.61
1.33	0.01	4.50	0.28	0.39
1.33	0.01	4.42	0.38	0.36
4.00	0.01	7.03	2.08	2.34
2.00	0.01	7.02	1.24	1.17
1.00	0.01	7.02	0.68	0.58
0.50	0.01	7.02	0.38	0.29
0.25	0.01	7.07	0.19	0.14
4.00	0.01	7.47	2.00	2.34
2.00	0.01	7.43	1.20	1.17
1.20	0.01	7.43	0.69	0.70
1.00	0.01	7.06	0.51	0.58
1.00	0.01	7.06	0.55	0.58
0.80	0.01	7.46	0.59	0.46
0.40	0.01	7.47	0.25	0.23

[a] At 15 °C and 0.1 M KCl. [b] $\gamma_H = 0.82$.

Ni(bpy) concentration for each of the three different total Ni(II) concentrations. Figure 2b shows the near-linear dependence of $1/\tau$ upon pH.

Any mechanism proposed for this system should be consistent with the following observations: (1) the effect is observed only when Ni(II), ATP, and bpy are present simultaneously; (2) the experimental $1/\tau$ values are very sensitive to initial metal ion concentration (Figure 2a) and pH (Figure 2b); (3) the thermodynamically dominant species are known[18] to be Ni(ATP), Ni(ATPH), Ni(ATP)(bpy), and HONi(ATP).

Near pH 6 the ternary relaxation data are consistent with a kinetic expression based on step 3–4 in Scheme II: Ni(ATP) + bpy = Ni(ATP)(bpy). This is not surprising given the mixing conditions of the experiment and the stability constant of Ni(ATP). However, a mechanism consisting of only the slow step 3–4 in Scheme II does not account for the continued increase in the experimental $1/\tau$ values *above* pH 6 apparent in Figure 2b. The increase of $1/\tau$ also cannot be explained by local aggregation or precipitation, since these would be expected to decrease $1/\tau$ by depleting the total aqueous Ni(II) concentration.

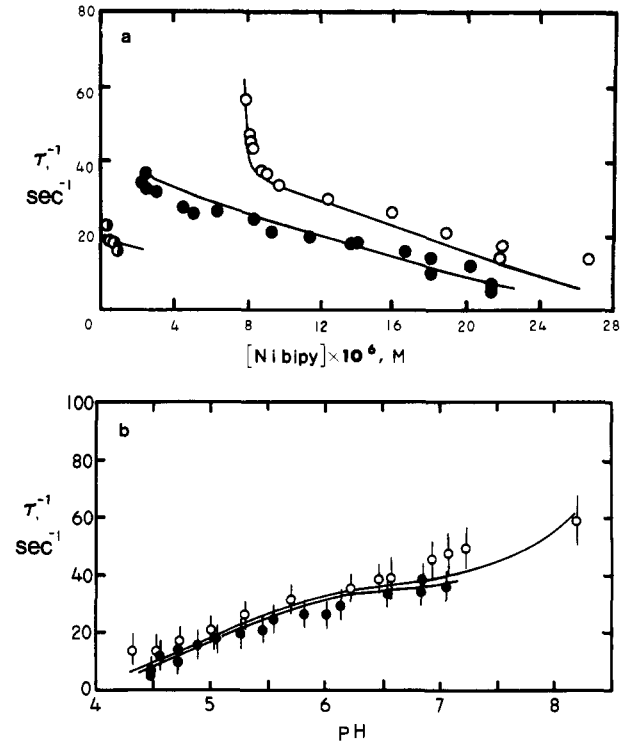

Figure 2. Variation of the reciprocal relaxation time ($1/\tau$) with pH, $[Ni]_0$ and $[bpy]_0$ for $[ATP]_0$ = 10 mM: (a) plotted vs. the equilibrium concentration of Ni(bpy) (see footnote 28); (b) plotted vs. pH. The different curves result from different overall metal ion concentrations: (○) 11.8 mM; (●) 9.4 mM; (◑) 4.0 mM (part a only). Experimental data points are indicated with circles; the solid line is calculated from eq 4.

Scheme II

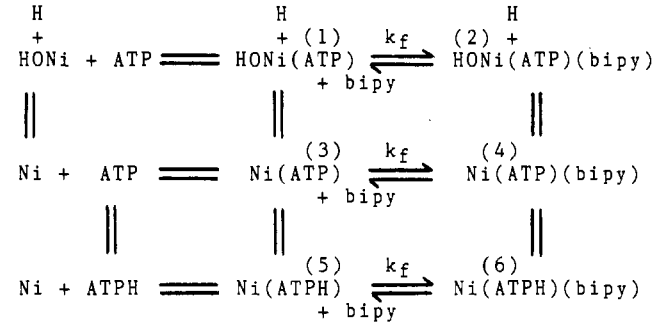

In order to model the trend of the data at high pH, four different hydroxo complexes (NiOH, HONi(ATP), HONi(bpy), and HONi(ATP)(bpy)) were considered in various pathways. Only the reaction HONi(ATP) + bpy = HONi(ATP)(bpy) (step 1–2 in Scheme II) coupled to step 3–4 reproduced the high pH end of the kinetic data, resulting in a 30% reduction in χ^2. To account for experimental data between pH 4 and 6, a third ternary formation pathway, step 5–6, has been included. This step further reduced χ^2 by 14%.

The complete mechanism for Ni|ATP|bpy, shown in Scheme II, includes three "slow" ternary complex formation steps, which are coupled by fast proton-transfer reactions. These proton transfers may be treated as preequilibria with the result that a single relaxation effect is predicted. The kinetic expression derived from Scheme II quantitatively reproduces the experimental data and is of the form

$$1/\tau = k_f^{12} f(c_1) + k_f^{34} f(c_2) + k_f^{56} f(c_3) \qquad (4)$$

where k_f^{ij} refers to the forward rate constants for the three slow steps and the $f(c)$ functions are complicated expressions involving

Scheme III

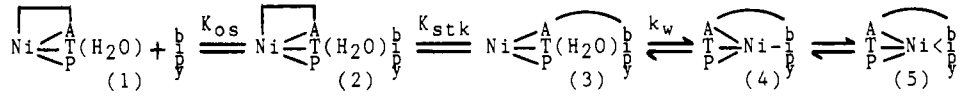

Table III. Relaxation Times for the Interaction of Ni(ATP) with bpy[a]

				$1/\tau$, s^{-1}	
$[Ni]_0$, mM	$[ATP]_0$, mM	$[bpy]_0$, mM	pH[b]	exptl	calcd
9.4	10.0	0.050	7.06	35.9	34.1
9.4	10.0	0.050	6.85	38.5	33.2
9.4	10.0	0.050	6.02	26.3	30.2
9.4	10.0	0.050	5.56	24.7	26.6
9.4	10.0	0.050	5.26	19.8	22.6
9.4	10.0	0.050	5.04	18.2	18.6
9.4	10.0	0.050	4.72	14.1	11.9
9.4	10.0	0.050	4.56	11.9	8.8
11.8	10.0	0.050	8.20	58.7	63.8
11.8	10.0	0.050	7.23	49.5	37.8
11.8	10.0	0.050	7.08	47.5	36.8
11.8	10.0	0.050	6.94	45.6	36.1
11.8	10.0	0.050	6.58	39.1	34.9
11.8	10.0	0.050	6.47	38.5	34.5
11.8	10.0	0.050	6.23	35.3	33.8
11.8	10.0	0.050	5.71	31.5	30.7
11.8	10.0	0.050	5.30	26.5	25.6
11.8	10.0	0.050	5.01	21.0	20.0
11.8	10.0	0.050	4.73	17.3	13.6
11.8	10.0	0.050	4.32	13.8	5.4
9.4	10.0	0.050	6.84	34.3	33.2
9.4	10.0	0.050	6.55	33.5	32.2
9.4	10.0	0.050	6.14	29.4	30.8
9.4	10.0	0.050	5.82	26.6	29.0
9.4	10.0	0.050	5.46	21.0	25.5
9.4	10.0	0.050	5.07	17.8	19.2
9.4	10.0	0.050	4.72	10.0	11.9
9.4	10.0	0.050	4.48	6.9	7.2
9.4	10.0	0.050	4.48	5.2	7.2
9.5	10.0	0.050	4.53	13.8	8.5
9.5	10.0	0.050	4.89	15.7	14.7
4.0	9.8	0.025	7.06	23.1	17.8
4.0	9.5	0.050	7.03	18.7	17.7
4.0	9.5	0.075	7.07	18.2	17.6
4.0	9.5	0.100	7.07	15.8	17.5

[a] At 15 °C and I = 0.1 M KCl. [b] γ_H = 0.82.

equilibrium concentrations. The solid lines in Figure 2 represent the $1/\tau$ points calculated from eq 4. These calculated points are presented in Table III along with their corresponding experimental conditions. Many other pathways and arrangements of pathways were modeled and rejected because the results were inconsistent or their contribution was not significant.

We obtained the pK_a values for Ni(ATPH)(bpy) = Ni(ATP)(bpy) + H^+ (step 6–4) and Ni(ATP)(bpy) = HONi(ATP)(bpy) + H^+ (step 4–2) as a result of the fitting process. The best-fit pK_a of 2.5 for the former reaction compares well with the known values of the CTP and ITP analogues.[18] χ^2 is not greatly sensitive to the value of pK_a for Ni(ATP)(bpy) = HONi(ATP)(bpy) + H^+, although the fit requires that a finite concentration of HONi(ATP)(bpy) exists. Previous thermodynamic studies[18,29] of this ternary system preclude a pK_a less than about 8, and we find a broad minimum in χ^2 for a pK_a value of about 10.

Discussion

The rates of binary metal complex formation are primarily dependent on the nature of the metal ion rather than that of the ligand.[30,31] For ternary systems it is often the reactant *metal complex* that determines the reaction rate constant.[6-8,32] This is expected when water dissociation is the rate-determining step. In those cases where a forward rate constant is smaller than the water exchange rate constant of the reactant complex, we conclude that some other process is rate-limiting, for example intracomplex ring closure or reactant rearrangement.

The forward rate constants resulting from our study of Ni|ATP|bpy can each be qualitatively understood in terms of Scheme III, which describes the complex formation interactions in more detail than is shown in Scheme I or II. Scheme III shows an outer-sphere association step, followed by a Ni|ATP + bpy stacking interaction, followed by a two-step inner-sphere chelation of bpy. The resulting kinetic expression is

$$k_{eff} = k_w K_{stk}/(1 + F) \quad (5)$$

where k_w is the water exchange rate constant for a reactant metal complex and F is the chelation rate constant ratio[33] k_w/k_{45} (see Scheme III). The quantity k_w for several relevant metal complexes has been determined by ^{17}O NMR.[2,34] The stability constant K_{stk} refers to a stacking equilibrium in which bpy interacts with Ni|ATP prior to the rate-determining step (RDS). In the context of the present work, this is envisioned to be a charge-transfer interaction between the adenosine ring of Ni(ATP) and bpy.

The factors K_{stk} and $1 + F$ in eq 5 obviously have opposing influences upon k_{eff}, which in turn is a component of the k_f values calculated by using eq 3 and 4. Three limiting possibilities are evident. In the simplest case (where $F << 1$ and stacking is not important so that K_{stk} may be replaced by unity) eq 5 predicts that k_{eff} will equal the water exchange rate constant (k_w). If $1 + F$ is greater than K_{stk}, then eq 5 predicts that k_{eff} will be less than k_w. Finally, if $1 + F$ is less than K_{stk} then eq 5 predicts that k_{eff} will be greater than k_w.

Binary (Ni|bpy). The values of K_{os}, S, and k_{eff} for Ni(II) + bpy are given in Table IV. In eq 2 we assume that $S_M = 1$ for the six equivalent[34] exchanging water molecules in $Ni(H_2O)_6$, and $S_L = 0.5$ for bpy. Scheme III and eq 5, therefore, are not directly applicable to this system in which the reactant metal complex is just $Ni(H_2O)_6$. For this simple system eq 5 correctly relates k_{eff}, k_w, and F only when K_{stk} is set to unity. This removes the contribution to eq 5 from the bpy|ATP stacking interaction described for the ternary systems. In this way we calculate F to be ca. 1, using the modified eq 5 and the values of k_{eff} and k_w in Table IV. A value of $F << 1$ indicates no contribution from a ring-closure step. The calculated value of F is small and near the anticipated limit of accuracy for this calculation; however, we conclude that the forward reaction rate constant for Ni(II) + bpy is consistent with the involvement of chelation ring closure and water dissociation in the RDS. We agree with the finding of Wilkins and co-workers,[3] who note that the first water dissociation is the *dominant* factor in determining the formation rate constant. We suggest, however, that the small value of k_f for Ni(II) + bpy relative to other Ni(II) systems, which they attributed to a decrease of K_{os} for Ni(II) + bpy, is due in part to chelation effects.

Ternary (Ni|ATP|bpy). There has been much experimental work and speculation concerning the structure and configuration of ternary complexes similar to Ni(ATP)(bpy). This structural information is useful in the estimation of the value of S and in the derivation of eq 5; therefore, this information will be summarized prior to the kinetic discussion for each of the three ternary products.

(1) Ni(ATP)(bpy). An X-ray diffraction study[35] has determined the solid-phase structure of $Zn(ATPH_2)(bpy)$. Powder

(29) Sigel, H. *J. Am. Chem. Soc.* **1975**, *97*, 3209–14.
(30) Eigen, M.; Tamm, K. *Z. Elektrochem.* **1962**, *66*, 93–106, 107–121.
(31) Ducommun, Y.; Newman, K. E.; Merbach, A. E. *Inorg. Chem.* **1980**, *19*, 3696–703.
(32) Sharma, V. S.; Leussing, D. L. "Metal Ions in Biological Systems"; Sigel, H., Ed.; Marcel Dekker: New York, 1974; Vol. 2, pp 127–66.
(33) Pasternack, R. F.; Sigel, H. *J. Am. Chem. Soc.* **1970**, *92*, 6146–51.
(34) Neely, J. W.; Connick, R. E. *J. Am. Chem. Soc.* **1972**, *94*, 3419–24.
(35) Orioli, P.; Cini, R.; Donati, D.; Mangani, S. *J. Am. Chem. Soc.* **1981**, *103*, 4446–52.

Table IV. Formation Rate Constants and Related Parameters

reaction	k_f(15 °C), M^{-1} s^{-1}	S^a	K_{os},[b] M^{-1}	k_{eff}, s^{-1}	k_w, s^{-1}
Ni + bpy (k_f) ⇌ Ni(bpy)	5.9×10^2	0.50	0.108	6×10^3	14×10^3 [c]
Ni(ATPH) + bpy (k_{12}) ⇌ Ni(ATPH)(bpy)	1.9×10^3	0.25	0.054	4×10^4	*e*
Ni(ATP) + bpy (k_{34}) ⇌ Ni(ATP)(bpy)	4.3×10^3	0.17	0.036	1×10^5	7×10^4 [d]
HONi(ATP) + bpy (k_{56}) ⇌ HONi(ATP)(bpy)	2.2×10^5	0.10	0.011	2×10^7	*e*

[a] The parameter S is defined by $S_M S_L$; see eq 2. [b] K_{os} is calculated with a = 3.5 Å in eq 2. [c] Reference 51. [d] Estimated from k_w for Mn(ATP) and $Mn(H_2O)_6$; see ref 41. [e] Unknown.

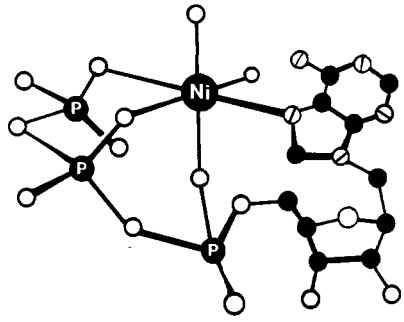

Figure 3. Proposed structure for Ni(ATP), see text: (●) carbon; (⊖) nitrogen; (○) oxygen.

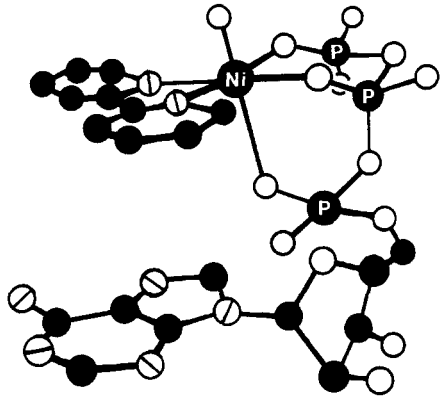

Figure 4. Proposed structure for Ni(ATP)(bpy), see text: (●) carbon; (⊖) nitrogen; (○) oxygen.

X-ray studies[36] for $M(ATPH_2)(bpy)$, where M = Zn(II), Mn(II), and Co(II),[37] show that these compounds "...are strictly isomorphous and can therefore be assumed to have essentially the same structure."[36] The crystal structure of $Ni(ATPH_2)(bpy)$ is probably similar to that for the Co(II) complex. This X-ray study and several solution studies[29,38] of the ternary complex demonstrate the presence of (ATP)(bpy) stacking, Ni(ATP) binding at the α-, β-, and γ-phosphate groups, and Ni(bpy) binding at N-2 and N-2′ (Figure 4). The stacking interaction disrupts[29,39] the inner-sphere[16,40] N-7 adenosine interaction with Ni(II), which is present in the binary Ni(ATP) complex shown in Figure 3.

A structure that is consistent with these findings is shown in Figure 4. This structure shows the adenosine ring of ATP stacked with bpy, and Ni(II) bound to the three phosphate groups of ATP in addition to the two nitrogen groups in bpy.

The effective forward rate consant (k_{eff}) for Ni(ATP) + bpy calculated from eq 5 is 1×10^5 s^{-1}; the corresponding value for Ni + bpy is 6×10^3 s^{-1}, indicating a labilization due to the presence of ATP bound to Ni(II). This comparison is more useful than a comparison of k_f values because k_{eff} is corrected for the different S values for the two reactions. The water exchange rate constant (k_w) for Ni(ATP) can be estimated from the known labilization ratio for water exchange in Mn(ATP) vs. Mn(II).[42] The resulting k_w for Ni(ATP) is ca. 7×10^4 s^{-1} at 15 °C. This value compares surprisingly well with our calculated k_{eff} for Ni(ATP) + bpy, 1×10^5 s^{-1}. This result suggests that either (1) there is no rate-limiting rearrangement step for Ni(ATP) + bpy, contrary to previous reports for Mn(II) ion,[42-44] or (2) $1 + F$ is approximately equal to K_{stk} for the reaction Ni(ATP) + bpy.

The stability of the stacking interaction (K_{stk}) may be estimated to be ca. 10 M^{-1};[45] however, this only places some constraints on the magnitude of F if the latter possibility (2) applies. On the basis of the Ni(ATP) + bpy data alone we cannot distinguish between these two possibilities.

(2) Ni(ATPH)(bpy). In Ni(ATPH)[46,47] and Ni(ATPH)-(bpy),[18,20] protonations of ATP occur at both the γ-phosphate and the adenosine ring at N-1. The ionization constants for these two protonated sites are very similar, resulting in a mixture of singly protonated complexes. Several studies have also found that stacking is present in $M(ATPH_2)(bpy)$[35,36] as well as in Ni-(ATP)(bpy); consequently, stacking is indicated for Ni-(ATPH)(bpy). The magnitude of the stacking interaction, however, is reduced[18] by protonation of the adenosine ring of Ni(ATP).

Our kinetic results for Ni(ATPH) + bpy show a reduced value of k_f as compared to that for Ni(ATP) + bpy. This is even more evident in the k_{eff} values. It is not likely that this reduction of k_{eff} for the protonated relative to the nonprotonated complex is due to an increase of F (see eq 5). Rather, if F varies, we expect that the magnitude of F would be reduced, because Ni(ATPH) is probably *more* accessible to bpy than is Ni(ATP). It is more probable that the reduction of k_{eff} for Ni(ATP) + bpy is due to the reduction of the extent of (HATP)(bpy) stacking in Ni-(ATPH)(bpy) (K_{stk} in Scheme III) relative to K_{stk} for (ATP)(bpy) in Ni(ATP)(bpy). The decrease in k_{eff} for Ni(ATP) may also be partially the result of a delabilization of k_w caused by the decreased charge on the bound γ-phosphate in Ni(ATPH) relative to Ni(ATP).

(3) HONi(ATP)(bpy). Two possible structures exist for the complex HONi(ATP)(bpy): (1) a structure similar to that shown in Figure 4 with the hydroxo ligand bound to Ni(II) in place of the remaining water molecule shown in Figure 4; or (2) an outer-sphere (ATP)(bpy) stacking complex in which the bpy is not bound to Ni(II).[48] The species HONi(ATP)(bpy) has not to our knowledge been previously detected.

Our kinetic data strongly suggest that a hydroxo "ternary" complex is formed, which is kinetically fully coupled to a parallel

(36) Cini, R.; Orioli, P. *J. Inorg. Biochem.* **1981**, *14*, 95–105.
(37) Note however that $Cu(ATPH_2)(bpy)$ appears to have a somewhat different structure according to ref 36.
(38) Naumann, C. F.; Sigel, H. *J. Am. Chem. Soc.* **1974**, *96*, 2750–6.
(39) Sigel, H. *J. Inorg. Nucl. Chem.* **1977**, *39*, 1903–11.
(40) Lam, Y.-F.; Kuntz, G. P. P.; Kotowycz, G. *J. Am. Chem. Soc.* **1974**, *96*, 1834–39.
(41) We assume $k_{w(Ni(ATP))} = k_{w(Ni(H_2O)_6)} k_{w(Mn(ATP))} / k_{w(Mn(H_2O)_6)}$ where $k_{w(Ni(ATP))} = 3.4 \times 10^4$ s^{-1} (25 °C, ref 51), $k_{w(Mn(ATP))} = 2.3 \times 10^7$ s^{-1} and $k_{w(Mn(H_2O)_6)} = 5.0 \times 10^7$ s^{-1}. The manganese water exchange data are from the results of: Zetter, M. S.; Lo, G. Y.-S.; Dodgen, H. W.; Hunt, J. P. *J. Am. Chem. Soc.* **1978**, *100*, 4430–6.
(42) Zetter, M. S.; Dodgen, H. W.; Hunt, J. P. *Biochemistry* **1973**, *12*, 778–82.
(43) Sternlicht, H.; Shulman, R. G.; Anderson, E. W. *J. Chem. Phys.* **1965**, *43*, 3123–32. Sternlicht, H.; Shulman, R. G.; Anderson, E. W. *J. Chem. Phys.* **1965**, *43*, 3133–43.
(44) Hague, D. N.; Martin, S. R.; Zetter, M. S. *J. Chem. Soc., Faraday Trans. 1* **1972**, *68*, 37–46.
(45) K_{stk} here is defined as the stability constant of the stacking interaction between Ni(ATP) and bpy. This is probably close to the stability constant of ATP + bpy. Log $K_{(ATP)(bpy)}$ = 0.91 at 25 °C according to: Mitchell, P. R.; Sigel, H. *J. Am. Chem. Soc.* **1978**, *100*, 1564–70.
(46) Khalil, F. L.; Brown, T. L. *J. Am. Chem. Soc.* **1964**, *86*, 5113–7.
(47) Perrin, D. D.; Sharma, V. S. *Biochim. Biophys. Acta* **1966**, *127*, 35–41.
(48) Dr. Sigel has estimated K for HONi(ATP) + bpy = HONi(ATP)(bpy) to be 10–15 M^{-1} for such a complex if it should prove to exist (private communication).

pathway at lower pH. This is apparent in the virtually linear dependence of $1/\tau$ upon pH between pH 6 and 8 (Figure 2b).

The large k_f and k_{eff} rate constants, which we calculate for HONi(ATP) + bpy (step 1-2 in Scheme II), indicate that the hydroxo ligand labilizes k_w and the Ni(II) + N-7 adenosine interaction in HONi(ATP). The increase of k_f could also be explained in part by an increase in K_{stk} for HONi(bpy).

If bpy is bound outer sphere in the HONi(ATP)(bpy) complex, then steps 4 and 5 in Scheme III would not be applicable and the formation rate would be independent of the rate of water dissociation. This could account for the large increase of k_f for HONi(ATP)(bpy) relative to k_f for Ni(ATP)(bpy).

In the absence of other information, Scheme III is preferred for HONi(ATP) + bpy because it is consistent with the variations of all three ternary rate constants. Furthermore, there is some precedent (from binary trivalent metal complexes)[49,50] for rate constant increases of the magnitude calculated by eq 5 for the hydroxo ternary complex (see k_{eff} in Table IV).

Conclusions

We have examined the formation kinetics of the Ni(II) + bpy and Ni|ATP + bpy systems and found that each exhibits one relaxation effect. The rate constant of the former is within a factor of 2 of the value predicted if the RDS is water dissociation. This reduction of k_f is consistent with a small involvement of the chelation ring-closure step in the RDS.

The ternary relaxation rate increases nearly linearly with increasing pH over our entire pH range. We have quantitatively modeled this behavior with a mechanism that includes three parallel ternary formation steps, which differ by the degree of protonation.

We conclude that charge donation from the hydroxo ligand, and to a lesser extent from the phosphate groups of ATP, results in a labilization of the remaining metal-bound water molecules and thus increases the forward rate constant. This trend dominates all other variations within this series of reactions. A secondary trend may be due to an interaction prior to the dissociation of water from the binary complex (the RDS) in which bpy stacks with ATP but is not bound to the metal ion. The stability of this interaction appears to be enhanced in HONi(ATP) + bpy and decreased in Ni(ATPH) + bpy relative to Ni(ATP) + bpy.

This is one of a small number of investigations that have studied the kinetics of ternary systems over a wide range of conditions. The collection of data over a wide range of pH has allowed ternary protonated and hydroxylated pathways for the Ni|ATP|bpy system to be characterized for the first time.

Acknowledgment. This work was supported by the NIH in the form of a research grant to J.E.S. (GM-13,116). We thank Dr. Ronald Nohr (Kimberly-Clark, Inc., Atlanta, GA) for his assistance in the early stages of data modeling and Dr. Helmut Sigel (Institute for Inorganic Chemistry, University of Basel, Basel, Switzerland) for helpful comments and the donation of software that proved useful in the ternary equilibrium calculations.

Registry No. ATP, 56-65-5; bpy, 366-18-7; Ni, 7440-02-0.

(49) Gouger, S.; Stuehr, J. *Inorg. Chem.* **1974**, *13*, 379-84.
(50) Miceli, J.; Stuehr, J. *J. Am. Chem. Soc.* **1968**, *90*, 6967-72.
(51) Bechtold, D. B.; Liu, G.; Dodgen, H. W.; Hunt, J. P. *J. Phys. Chem.* **1978**, *82*, 333-7.

Contribution from the Department of Chemistry, Princeton University, Princeton, New Jersey 08544, and Department of Biochemistry, University of Georgia, Athens, Georgia 30602

Resonance Raman Spectra of Rubredoxin: New Assignments and Vibrational Coupling Mechanism from Iron-54/Iron-56 Isotope Shifts and Variable-Wavelength Excitation

Roman S. Czernuszewicz,† Jean LeGall,‡ Isabel Moura,‡ and Thomas G. Spiro*†

Received September 24, 1985

Resonance Raman spectra are reported for rubredoxin from *Desulfovibrio gigas* in frozen solution (77 K) with excitation by several lines of Ar^+ and Kr^+ lasers, from 488.0 to 568.2 nm. The use of low-temperature and variable-wavelength excitation has provided more complete spectra than were hitherto available, and several new bands are reported. All three components of the $\nu_3(T_2)$ asymmetric Fe-S stretching mode of the FeS_4 tetrahedron have been identified with the aid of ^{54}Fe substitution, at 376, 366, and 348 cm^{-1}. The isotope shifts, 1.1-2.5 cm^{-1}, are smaller than expected for the asymmetric vibrations and reveal that the component modes are vibrationally coupled to other modes of the cysteine ligands, most probably involving SCC bending. The previous assignment of one of the ν_3 components to a band at 324 cm^{-1} is excluded by its lack of isotope shift; most likely this band contains one or more of the coupled SCC modes. Numerous overtone and combination bands of the Fe-S stretches are observed, and a band at 653 cm^{-1} is assigned to a C-S stretching mode. The $\nu_2(E)$ and $\nu_4(T_2)$ SFeS bending modes are located at 130 and 150 cm^{-1}. The ν_2 band is enhanced with 4965-Å excitation, and its intensity is suggested to arise via its A_1 component in the effective optical symmetry, D_{2d}, of the chromophore. In contrast, the ν_4 mode is enhanced at 5682 Å, and it appears to be depolarized; a vibronic enhancement mechanism is suggested whereby the E component of this mode mixes the locally resonant $^6B_2$ charge-transfer excited state with the nearby ^6E state. A similar intensity variation of the ν_3 components suggests that the 376-cm^{-1} band represents the asymmetric Fe-S stretch oriented along the D_{2d} symmetry axis, while the other two bands arise from the perpendicular vibrations.

Introduction

Rubredoxin is the simplest member of the iron-sulfur proteins,[1] containing a single high-spin Fe^{III} ion, which undergoes reversible one-electron reduction at a potential close to -0.05 V.[2] The X-ray crystal structure of oxidized protein from *Clostridium pasteurianum* has been determined to a resolution of 1.2 Å.[3] The Fe^{III} ion is coordinated by four cysteine side chains, in a tetrahedral arrangement. Although one of the Fe-S bonds was initially found to be anomalously short,[4] subsequent refinement has removed the anomaly; all of the Fe-S distances are within experimental error of the mean value, 2.29 Å. The Fe-K edge EXAFS spectrum[5]

* To whom correspondence should be addressed.
† Princeton University.
‡ University of Georgia.

(1) Spiro, T. G., Ed. "Iron-Sulfur Proteins"; Wiley-Interscience: New York, 1982.
(2) Eaton, W. A.; Lovenberg, W. In "Iron-Sulfur Proteins"; Lovenberg, W., Ed.; Academic Press: New York, 1973; Vol. 2, Chapter 3.
(3) Watenpaugh, K. D.; Sieker, L. C.; Jensen, L. H. *J. Mol. Biol.* **1979**, *131*, 509-522.
(4) Watenpauch, K. D.; Sieker, L. C.; Herriott, J. R.; Jensen, . H. *Acta Crystallogr., Sect. B: Structur. Crystallogr. Cryst. Chem.* **1973**, *29B*, 943-956.

0020-1669/86/1325-0696$01.50/0